Monthly Notices
of the
ROYAL ASTRONOMICAL SOCIETY

Mon. Not. R. Astron. Soc. **416,** 383–390 (2011) doi:10.1111/j.1365-2966.2011.19039.x

Formation rates of star clusters in the hierarchical merging scenario

R. Smith,[1]★ R. Slater,[1] M. Fellhauer,[1] S. Goodwin[2] and P. Assmann[1]

[1]*Departamento de Astronomia, Universidad de Concepcion, Casilla 160-C, Concepcion, Chile*
[2]*Department of Physics and Astronomy, University of Sheffield, Hicks Building, Hounsfield Road, Sheffield S3 7RH*

Accepted 2011 May 10. Received 2011 April 28; in original form 2011 March 28

ABSTRACT

Stars form with a complex and highly structured distribution. For a smooth star cluster to form from these initial conditions, the star cluster must erase this substructure. We study how substructure is removed using *N*-body simulations that realistically handle two-body relaxation. In contrast to previous studies, we find that hierarchical cluster formation occurs chiefly as a result of scattering of stars out of clumps, and not through clump merging. Two-body relaxation, in particular within the body of a clump, can significantly increase the rate at which substructure is erased beyond that of clump merging alone. Hence the relaxation time of individual clumps is a key parameter controlling the rate at which smooth, spherical star clusters can form. The initial virial ratio of the clumps is an additional key parameter controlling the formation rate of a cluster. Reducing the initial virial ratio causes a star cluster to lose its substructure more rapidly.

Key words: stars: formation – galaxies: star clusters: general.

1 INTRODUCTION

The vast majority of stars do not form alone. They appear to form in a hierarchy in structures of tens to tens of thousands of stars (Testi et al. 2000; Gutermuth et al. 2005; André et al. 2007; Sánchez, Alfaro & Pérez 2007; Goldsmith et al. 2008; Gutermuth et al. 2009; André et al. 2010; Bressert et al. 2010; di Francesco et al. 2010; Gouliermis et al. 2010). Such structures are a natural consequence of the gravoturbulent model of star formation (e.g. Klessen & Burkert 2000; Bonnell et al. 2001; Bonnell, Bate & Vine 2003; Bate, Bonnell & Bromm 2003; Bonnell, Clark & Bate 2008; Bate 2009; Offner, Hansen & Krumholz 2009).

Hierarchical distributions are not in equilibrium, and will rapidly dynamically evolve into dense star clusters or loose associations (e.g. Aarseth & Hills 1972; Bate, Clarke & McCaughrean 1998; Goodwin 1998; Boily, Clarke & Murray 1999; Kroupa & Bouvier 2003; Goodwin & Whitworth 2004; Allison et al. 2009, 2010; Moeckel & Bonnell 2009; Fellhauer, Wilkinson & Kroupa 2009; Gieles, Sana & Portegies Zwart 2010). Such evolution is especially violent if the stars are initially dynamically cool (see Allison et al. 2009, 2010) as many observations suggest they are (e.g. Di Francesco, André & Myers 2004; Walsh, Myers & Burton 2004; Peretto, André & Belloche 2006; André et al. 2007; Kirk, Johnstone & Tafalla 2007; Walsh et al. 2007; Gutermuth et al. 2008).

In a clustered phase, many interesting processes may occur such as rapid dynamical mass segregation (Allison et al. 2009, 2010), binary disruption and modification (Heggie 1974; Kroupa 1995; Parker et al. 2009), the formation of high-order multiples like the Trapezium system (Aarseth, Henon & Wielen 1974; Zinnecker 2008; Allison et al. 2010) and star–disc interactions affecting planetary system formation (Boffin et al. 1998; Watkins et al. 1998; Pfalzner et al. 2005; Thies, Kroupa & Theis 2005; Thies et al. 2010). Therefore, an understanding of the collapse of hierarchical distributions is important to understand the formation of star clusters and the possible importance of these effects.

The evolution of initially substructured stellar distributions into smooth star clusters has been studied by many authors (e.g. Aarseth & Hills 1972; Goodwin 1998; Boily et al. 1999; Kroupa & Bouvier 2003; Goodwin & Whitworth 2004; Allison et al. 2009; Fellhauer et al. 2009; Moeckel & Bonnell 2009; Smith et al. 2011). In particular, Fellhauer et al. (2009) attempted to quantify how rapidly an initially clumpy distribution could evolve into a smooth star cluster.

In this paper, we particularly extend the work of Fellhauer et al. (2009) and Smith et al. (2011) to investigate how a collapsing clumpy distribution in a static gas potential is able to erase its substructure and form a smooth cluster. Fellhauer et al. (2009) presented a semi-analytic model for the erasure of substructure, but they did not properly account for two-body effects in their simulations. Here we revisit their analysis with an accurate *N*-body code.

In Section 2 we present our initial conditions, in Section 3 we study the erasure of substructure before examining the rates at which substructure is erased in Section 4. Finally, we discuss our results in Section 5, and draw our conclusions in Section 6.

★E-mail: rsmith@astro-udec.cl

2 INITIAL CONDITIONS

We perform our N-body simulations using the direct N-body >integration code NBODY6 (Aarseth 2003). The advantage of NBODY6 is that it is able to rapidly and accurately model stellar dynamics, and two-body encounters in particular.

Our initial conditions are similar to those of Fellhauer et al. (2009, hereafter F09). Our young star-forming regions have a total mass of $1000\,\mathrm{M}_\odot$. We assume they convert gas to stars with an efficiency ϵ which ranges between 0.1 and 0.8. Therefore, the mass of stars is $\epsilon \times 1000\,\mathrm{M}_\odot$, and the mass of gas $(1-\epsilon) \times 1000\,\mathrm{M}_\odot$.

We simulate the gas with a static background Plummer potential with a Plummer scale radius of $R_{\rm pl}^{\rm sc}$ which ranges between 0.02 and 1 pc. We set a limiting cut-off radius for the gas potential of $5 \times R_{\rm pl}^{\rm sc}$. We acknowledge that this is not ideal, as the gas will also dynamically evolve. However, it is presently impossible to simply model live background gas and so we follow previous studies in including a static background (e.g. Moeckel & Bonnell 2009; F09; Smith et al. 2011).

The stars are distributed within the gas potential in N_0 subclumps which follow the underlying gas Plummer distribution. N_0 ranges from 4 to 32 resulting in a mass per clump of $M_{\rm pl} = 6$ to $80\,\mathrm{M}_\odot$ [where the clump stellar mass is $M_{\rm pl} = (\epsilon \times 1000)/N_0\,\mathrm{M}_\odot$].

Subclumps are distributed within the Plummer sphere according to the prescription of Aarseth et al. (1974). Their bulk velocities are then scaled to a desired virial ratio $Q_{\rm i} = T/|\Omega|$ (where T is the total kinetic energy and Ω the total potential energy), where $Q_{\rm i} = 0.5$ is virial equilibrium and our scaling ranges between $Q_{\rm i} = 0$ and 0.5.

Each clump is assumed to be a virialized Plummer sphere with a Plummer scale radius of $R_{\rm pl} = 0.01$ pc and a cut-off radius beyond which no stars are placed of $R_{\rm cut} = 5\,R_{\rm pl} = 0.05$ pc. We assume that subclumps are virialized initially as their relaxation time is so short that they will rapidly virialize (but this process is also effective at destroying clumps as we shall see).

We take equal-mass stars of mass $0.5\,\mathrm{M}_\odot$ (roughly the average mass of a star from a standard initial mass function). This means that our clumps contain from 12 to 160 stars depending on the values of ϵ and N_0. Again, we acknowledge that equal-mass stars are not realistic. In particular, differences in stellar masses will have a significant effect on two-body encounters which we are attempting to examine in particular detail. However, introducing a range of stellar masses would significantly increase stochasticity and add another free parameter, so we choose to ignore it for now.

Therefore the important parameters are

(i) star formation efficiency ϵ;
(ii) gas Plummer scale radius $R_{\rm pl}^{\rm sc}$;
(iii) number of subclumps N_0 and
(iv) virial ratio of the stellar distribution $Q_{\rm i}$.

From these parameters it is possible to calculate a number of very useful quantities.

The filling factor, α, is the fraction of the volume which contains subclumps:

$$\alpha = \frac{R_{\rm pl}}{R_{\rm pl}^{\rm sc}}. \quad (1)$$

The crossing time of the whole system, $T_{\rm cr}^{\rm sc}$, or of an individual clump, $T_{\rm cr}$, is the typical time taken to cross the whole system or individual clump (the typical size divided by the typical speed).

The two-body relaxation time is a measure of how rapidly the internal velocities of a clump will change by order of their own magnitude and is given by

$$t_{\rm relax} = 0.1 \frac{N_{\rm part}}{\ln(N_{\rm part})} t_{\rm cr}, \quad (2)$$

where $N_{\rm part}$ is the total number of particles in the system, and $t_{\rm cr}$ is the crossing time of the system.

A list of all the simulations and their parameters can be seen in Table 1. Three different random realizations of each parameter set are performed.

3 RESULTS

First, we shall examine in detail our 'standard model'. This is a virialized $Q_{\rm i} = 0.5$ cluster with a star formation efficiency of $\epsilon = 0.32$ and $N_0 = 16$. This cluster has a stellar mass of $320\,\mathrm{M}_\odot$ in 16 $20 = \mathrm{M}_\odot$ clumps (40 equal-mass stars per clump). The cluster has a filling factor of $\alpha = 0.05$ and a total crossing time of 260 kyr. Each clump has a crossing time of 20 kyr and a relaxation time of 22 kyr.

Fig. 1 shows the evolution of the standard model for 10 crossing times (2.6 Myr). Initially ($t = 0$ Myr), the stars have a highly clumpy and substructured distribution. By 0.5 Myr the initial structure is already less obvious, and by >1 Myr the cluster has a fairly smooth appearance with very little evidence of the initial clumps.

It is expected that the erasure of substructure would be due to one, some or all of the following mechanisms.

(i) Internal scattering and the ejection of stars from a clump by internal two-body interactions.
(ii) Tidal stripping of clumps by the gas potential.
(iii) Tidal encounters between clumps.
(iv) Collisions between clumps or stars.

An examination of Fig. 1 suggests that internal scattering is a crucial factor in the erasure of substructure. By 0.5 Myr, the appearance of the cluster is already quite smooth (we shall return later to quantify the erasure of substructure, but for now we will use a 'by eye' examination). In only two system crossing time interactions between clumps cannot have been important. The high density of the initial clumps also suggests that tidal stripping by other clumps or the gas potential cannot have been responsible for the smoothness. The only process that works so rapidly on clumps is internal relaxation as the clumps are 20 internal relaxation times old by 0.5 Myr.

The effect of internal relaxation is to eject stars from the clumps forming a smooth background of stars, and also to increase the size of the clumps ('puffing up'). The puffing-up of clumps is obvious in Fig. 1 where even isolated clumps at 0.5 Myr are clearly larger than initially. Binary formation within clumps is observed. This likely plays a significant role in enhancing scattering and ejection of stars from clumps.

As well as introducing a background of ejected stars, puffing-up has two effects which further increase the rate of clump mergers. As clumps are larger they are more susceptible to tidal stripping, and the filling factor increases – significantly increasing the rate of clump collisions.

In the clump merger simulations of F09, these effects arising from two-body encounters were missed as the SUPERBOX code used for these simulations damps two-body encounters entirely. This is illustrated in Fig. 2, showing two simulations with the same initial conditions[1] having evolved for 0.7 Myr (2.7 crossing times).

[1] It should be noted that the SUPERBOX runs have 10^5 much lower mass particles initially in each clump, and here we display only 40 for a fair comparison.

Table 1. A complete list of the parameters of all the simulations in our parameter study. The table is split by horizontal lines into sets (sets 1–6, from top to bottom). Each set is chosen to test the influence of a specific parameter on the formation rate of the cluster (see text for further details). Columns give the filling factor α, the star formation efficiency ϵ, number of clumps N_0, the Plummer radius $R_{\rm pl}^{\rm sc}$, the cut-off radius $R_{\rm cut}^{\rm sc}$, the total mass $M_{\rm pl}^{\rm sc}$ and the crossing time of the star-forming region $T_{\rm cr}^{\rm sc}$. The following two columns are initial virial ratio $Q_{\rm i}$ and corresponding velocity dispersion of clumps with respect to their clumps within the region $\sigma_{\rm 3D}^{\rm sc}$. The next two columns are the mass in stars $M_{\rm star}$ and mass in gas $M_{\rm gas}$ (modelled as an analytical background) within the star-forming region. Finally, we show the Plummer radius $R_{\rm pl}$, the cut-off radius $R_{\rm cut}$, the mass $M_{\rm pl}$, the crossing time $T_{\rm cr}$ and the relaxation time of an individual clump $t_{\rm relax}$.

α	ϵ	N_0	$R_{\rm pl}^{\rm sc}$ (pc)	$R_{\rm cut}^{\rm sc}$ (pc)	$M_{\rm pl}^{\rm sc}$ ($M_\odot$)	$T_{\rm cr}^{\rm sc}$ (kyr)	$Q_{\rm i}$	$\sigma_{\rm 3D}^{\rm sc}$ (km s^{-1})	$M_{\rm star}$ ($M_\odot$)	$M_{\rm gas}$ ($M_\odot$)	$R_{\rm pl}$ (pc)	$R_{\rm cut}$ (pc)	$M_{\rm pl}$ ($M_\odot$)	$T_{\rm cr}$ (kyr)	$t_{\rm relax}$ (kyr)
0.05	0.32	16	0.20	1.00	1000	260	0.5	2.5	320	680	0.01	0.05	20.0	20	21.7
0.05	0.32	16	0.20	1.00	1000	260	$0.\dot{3}$	2.0	320	680	0.01	0.05	20.0	20	21.7
0.05	0.32	16	0.20	1.00	1000	260	0.1	1.4	320	680	0.01	0.05	20.0	20	21.7
0.05	0.32	16	0.20	1.00	1000	260	0.0	0.0	320	680	0.01	0.05	20.0	20	21.7
0.01	0.32	16	1.00	5.00	1000	2950	0.5	1.1	320	680	0.01	0.05	20.0	20	21.7
0.02	0.32	16	0.50	2.50	1000	1043	0.5	1.6	320	680	0.01	0.05	20.0	20	21.7
0.10	0.32	16	0.10	0.50	1000	93	0.5	3.6	320	680	0.01	0.05	20.0	20	21.7
0.20	0.32	16	0.05	0.25	1000	33	0.5	5.0	320	680	0.01	0.05	20.0	20	21.7
0.50	0.32	16	0.02	0.10	1000	8	0.5	8.0	320	680	0.01	0.05	20.0	20	21.7
0.05	0.32	4	0.20	1.00	1000	260	0.5	2.5	320	680	0.01	0.05	80.0	10	31.5
0.05	0.32	8	0.20	1.00	1000	260	0.5	2.5	320	680	0.01	0.05	40.0	15	27.4
0.05	0.32	32	0.20	1.00	1000	260	0.5	2.5	320	680	0.01	0.05	10.0	29	19.4
0.05	0.10	16	0.20	1.00	1000	260	0.5	2.5	96	904	0.01	0.05	6.0	37	17.9
0.05	0.20	16	0.20	1.00	1000	260	0.5	2.5	200	800	0.01	0.05	12.5	26	20.2
0.05	0.25	16	0.20	1.00	1000	260	0.5	2.5	248	752	0.01	0.05	15.5	24	21.7
0.05	0.50	16	0.20	1.00	1000	260	0.5	2.5	496	504	0.01	0.05	31.0	17	25.5
0.05	0.60	16	0.20	1.00	1000	260	0.5	2.5	600	400	0.01	0.05	37.5	15	26.1
0.10	0.10	16	0.10	0.50	1000	93	0.5	3.6	96	904	0.01	0.05	6.0	37	17.9
0.10	0.20	16	0.10	0.50	1000	93	0.5	3.6	200	800	0.01	0.05	12.5	26	20.2
0.10	0.25	16	0.10	0.50	1000	93	0.5	3.6	248	752	0.01	0.05	15.5	24	21.7
0.10	0.50	16	0.10	0.50	1000	93	0.5	3.6	496	504	0.01	0.05	31.0	17	25.5
0.10	0.70	16	0.10	0.50	1000	93	0.5	3.6	696	304	0.01	0.05	43.5	14	26.1
0.05	0.80	32	0.20	1.0	1000	260	0.5	2.5	800	200	0.01	0.05	25.0	18	22.9
0.05	0.40	16	0.20	1.0	1000	260	0.5	2.5	400	600	0.01	0.05	25.0	18	22.9
0.05	0.20	8	0.20	1.0	1000	260	0.5	2.5	200	800	0.01	0.05	25.0	18	22.9

Therefore, it is worth revisiting the results of F09 when applied to star clusters in light of this vitally important physical process. We note that the F09 results apply to situations where two-body encounters can be considered negligible.

3.1 Clump counting with a minimum spanning tree

A minimum spanning tree (MST) is the shortest path linking a set of n points with no closed loops. The MST is useful in that it always has $n - 1$ connections (edges) with a unique total length [see e.g. Cartwright & Whitworth (2004) or Allison et al. (2009) for uses of the MST in astronomy]. We use the algorithm described in Allison et al. (2009) to construct an MST for a simulation at some point in time.

In order to identify clumps, we introduce a cutting length $l_{\rm cut}$. If an edge has a length greater than $l_{\rm cut}$, then it is removed and we examine the subset of connections remaining after cutting the longest edges. If a subset contains more than one-third of the stars initially within a subclump, then we define it as a clump. [Note that Gutermuth et al. (2009) use a similar method, as do many friends-of-friends clump finders.] However, we introduce an extra element as our clumps are not just close in physical space, but in phase space. Therefore, we build our MST in 6D phase space before applying the cut.

A significant problem with clump finding is that it can be very sensitive to the cutting length used. In our initial conditions, we have the luxury of knowing what clumps are present and where they are. This allows us to fine tune our cutting length to get the right answer initially (a bad choice of cutting length can result in garbage). We also check a number of simulations by eye to see that the structures selected as clumps are indeed clumps, and that no structure have been missed. This is not ideal, but the best we can do at the moment with no way of properly selecting a cutting length [Gutermuth et al. (2009) propose a way of selecting the cutting length, but this only works well when structures are distinct].

An illustration of the method is given in Fig. 3 which quantifies the evolution of the NBODY6 and SUPERBOX simulations illustrated in Fig. 2. The solid lines shows the rapid decrease in the number of clumps in the NBODY6 simulation compared to those in the SUPERBOX simulation in the dashed line. This agrees with the by eye assessment of the far more rapid erasure of substructure in the former simulation (Fig. 1).

4 A PARAMETER STUDY OF CLUSTER FORMATION RATES

With a quantitative measure of the evolution of the substructure and a better understanding and modelling of the physical processes

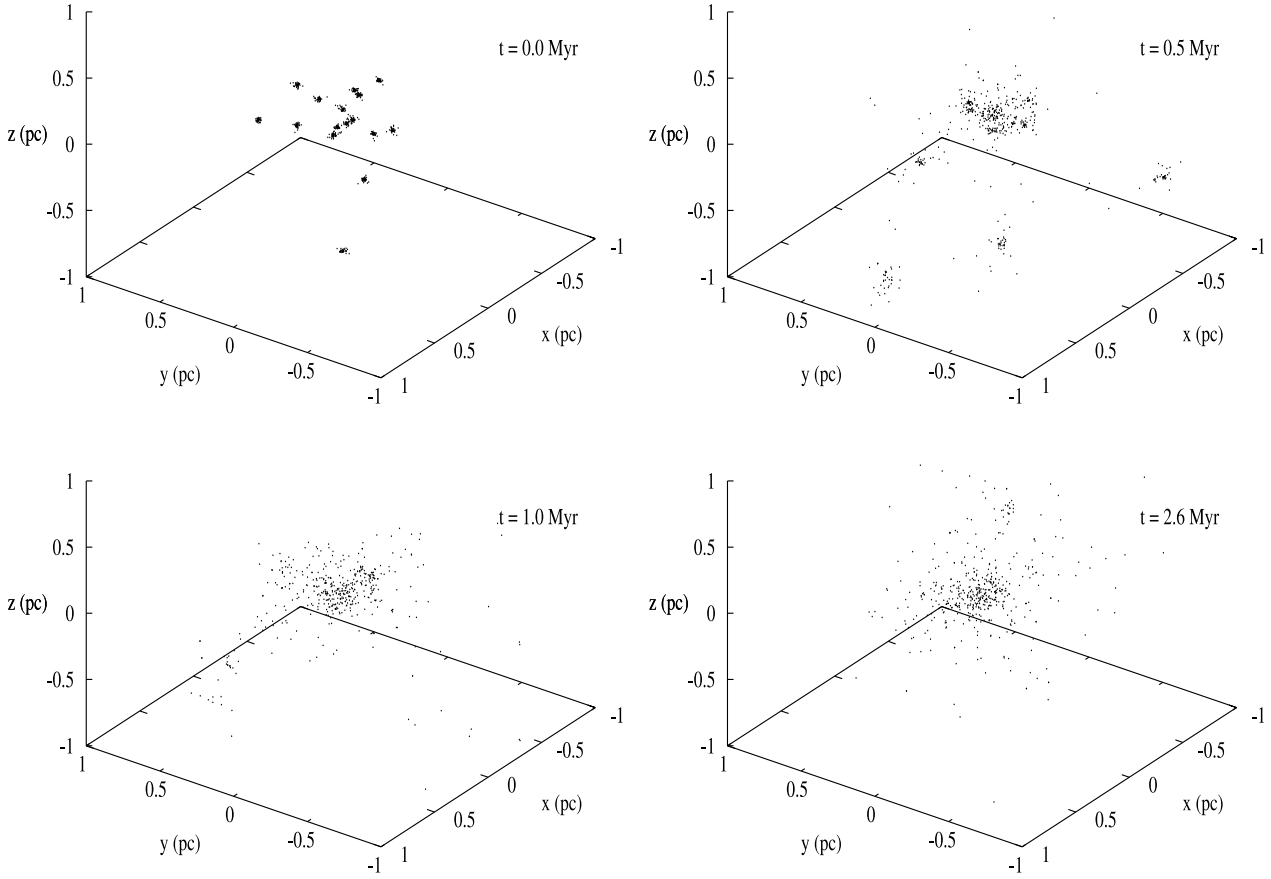

Figure 1. An *xyz*-plot of evolution of substructure in a standard model simulation. The upper-left panel shows the initial stellar distribution ($t = 0.0$ Myr). Stars are initially distributed in well-defined clumps. The standard model star-forming region has a crossing time $T_{\rm cr}^{\rm sc} = 260$ kyr. As the simulation evolves, we show snapshots at 2 (upper-right panel), 4 (lower-left panel) and 10 (lower-right panel) crossing times. Individual clumps 'puff up' significantly in less than two crossing times. By four crossing times, only a few clearly defined clumps are visible, and by 10 crossing times almost all substructure has been erased.

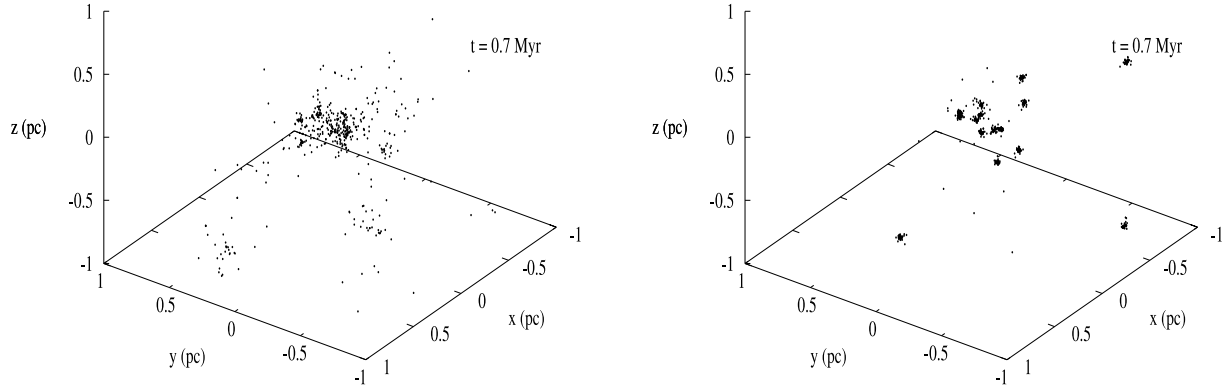

Figure 2. The resulting stellar distribution after 0.7 Myr of evolution from the standard model initial conditions in an NBODY6 simulation (left-hand panel) and a SUPERBOX simulation (right-hand panel). Substructure has been erased more rapidly in the NBODY6 simulations as a result of a realistic handling of two-body relaxation.

behind this erasure, we can revisit the study of F09 to quantify the rate at which structure is erased.

F09 suggested that the rate of erasure of substructure measured by the number of clumps at time τ, $N(\tau)$, compared to the initial number of subclumps, N_0, could be well fitted by an equation of the form:

$$N(\tau) = (N_0 - 1)\exp(-\eta\tau) + 1, \quad (3)$$

where η is a free parameter that depends on the initial conditions

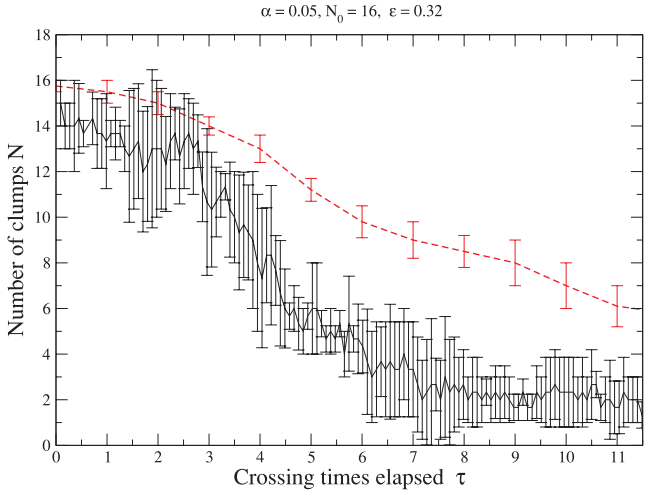

Figure 3. A graph of evolution of number of clumps N with time τ (in units of the star-forming region crossing time). Both curves are the results for simulations with the standard model initial conditions. The solid (black) line is the results for the NBODY6 run as measured using an MST based clump finder. The dashed (red) line is the results for the SUPERBOX run. As can be qualitatively assessed by eye in Fig. 2, substructure is more quickly erased in the NBODY6 simulations as a result of a realistic handling of two-body relaxation. Equivalently, the NBODY6 star cluster forms more rapidly.

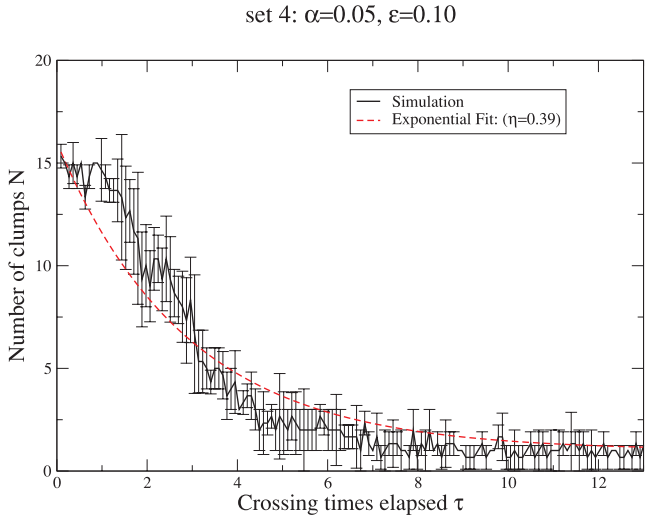

Figure 4. A graph of evolution of number of clumps N with time τ (in units of the star-forming region crossing time). The solid (black) curve is the results of a set 4 simulation as measured using the MST based clump finder. The dashed (red) line is an example of an exponential fit, using equation (3), to the simulation results. As presented in the key, this fit provides us with a value for the cluster formation rate parameter η. A high resulting value of η indicates that substructure has been erased rapidly, and thus that a smooth cluster has formed rapidly.

of the simulation. A large value of η corresponds to a rapid loss of substructure and the rapid appearance of a smooth cluster. Therefore we refer to η as the 'cluster formation rate'.

As shown in Fig. 4, we agree with F09 that an exponential decay is indeed a good fit to the rate at which substructure is lost.

4.1 Results of the parameter study on cluster formation rate

In Fig. 5 we show the variation of the cluster formation rate η with different parameters in our study (see Table 1). Please note the differing y-axis scales in the panels of Fig. 5. Remember also that each clump has the same size in each simulation.

4.2 The initial virial ratio Q_i

The upper-left panel of Fig. 5 shows how cluster formation rate depends on the initial virial ratio. As the initial virial ratio becomes increasingly subvirial (cool), the cluster formation rate steadily increases. This occurs as a result of increased clump–clump interactions – for subvirial initial conditions, clumps tend to fall into a more compact configuration within the gas potential. Cluster formation rate steeply rises as Q_i falls below 0.1. In this case, clumps tend to fall towards the centre of the gas potential well on time-scales $\sim$1 free-fall time, resulting in multiple simultaneous clump–clump collisions. *The initial virial ratio Q_i is a key parameter controlling the cluster formation rate*.

4.3 The filling factor α

The upper-right panel of Fig. 5 shows how cluster formation rate depends on the filling factor α. For $\alpha < 0.2$, the cluster formation rate is fairly constant as it is dominated by the ejection of stars from clumps rather than clump–clump interactions. However, for very high filling factors ($\alpha \sim 0.5$), the cluster formation rate becomes high. When filling factor is this high, clumps are almost overlapping in the initial conditions, and this is enhanced by clumps puffing up, hence rapid merging occurs.

4.4 The initial number of clumps N_0 and star formation efficiency ϵ

The middle-left panel of Fig. 5 shows how the cluster formation rate depends on the initial number of clumps N_0, and the middle-right panel shows how cluster formation rate depends on star formation efficiency ϵ. At a first glance, the cluster formation rate appears to depend on both N_0 and ϵ. A trend towards increasing cluster formation rate for increasing N_0 is visible in the middle-left panel. Meanwhile, as star formation efficiency falls, cluster formation rate increases. This trend is the reverse of what is seen in the F09 simulations.

However, by varying N_0 and ϵ we vary the initial number of stars in a clump. This results in a variation in the relaxation time $t_{\rm relax}$ of any individual clump and hence the speed at which clumps puff up (see sets 3 and 4 of Table 1). As N_0 increases, $t_{\rm relax}$ falls. Meanwhile, as ϵ increases, $t_{\rm relax}$ grows. Therefore, it is difficult to separate the additional effects of varying $t_{\rm relax}$ on cluster formation rate.

4.5 A fixed clump relaxation time $t_{\rm relax}$

In the bottom-left panel of Fig. 5, we show how the cluster formation rate varies for clumps with a fixed internal relaxation time (selecting values of N_0 and ϵ such that the relaxation time is 22.9 kyr). For a constant $t_{\rm relax}$, the cluster formation rate is roughly constant. This strongly suggests that it is the internal relaxation of clumps – the ejection of stars to make a background and the puffing up of clumps to enhance clump–clump collisions and tidal interactions that are the crucial physical parameters.

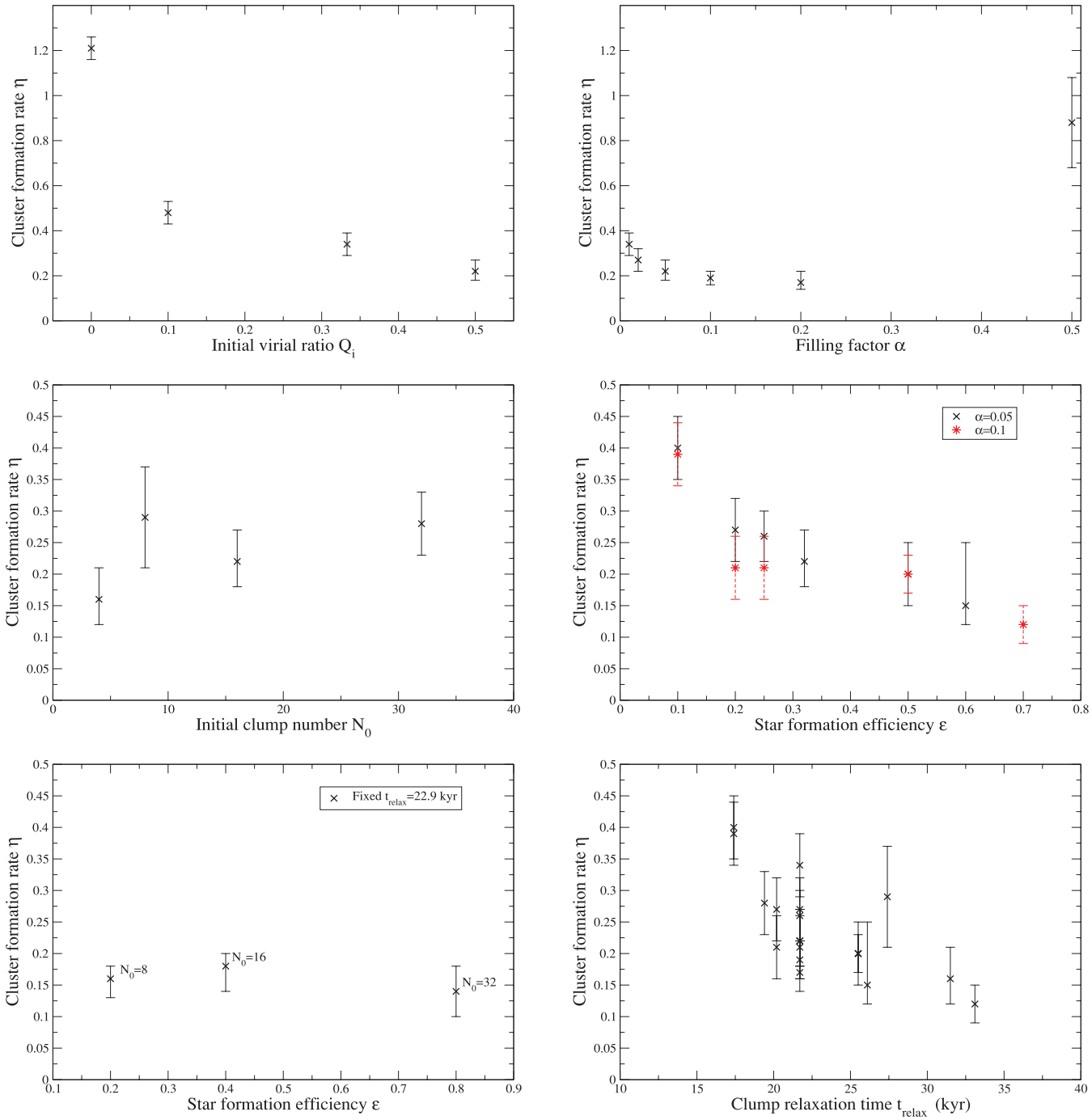

Figure 5. Plots of the dependency of the cluster formation rate parameter η (y-axis) versus the parameters investigated in the parameter study (x-axis), initial virial ratio Q_i, filling factor α (upper-right panel), the initial number of clumps N_0 (middle-left panel), region star formation efficiency ϵ (middle-right panel), region star formation efficiency ϵ for fixed clump relaxation time t_{relax} (bottom-left panel) and clump relaxation time t_{relax} (bottom-right panel). A description and discussion of these results is provided in the text (see Section 4.1). Please note the varying scale on y-axis. The two upper panels have a matching y-scale to each other. The four panels beneath them all have matching y-scale to each other.

4.6 The relaxation time of individual clumps

This conclusion is further supported by the bottom-right panel of Fig. 5 where the cluster formation rate can be seen to decrease with greater clump internal relaxation time. Note that these simulations are all for an initially virialized clump distribution, and we also exclude the $\alpha = 0.5$ filling factor simulation as the cluster formation times in these simulations are dominated by other effects. It appears that *the clump relaxation time is a key parameter controlling the cluster formation rate*.

5 DISCUSSION

As discussed in the introduction, star formation is a messy and complex process that does not initially produce a smooth, relaxed

star cluster. To give the roughly spherical, smooth star clusters that we often observe, substructure must be erased (see also Aarseth & Hills 1972; Goodwin 1998; Boily et al. 1999; Kroupa & Bouvier 2003; Goodwin & Whitworth 2004; Allison et al. 2009; F09).

The speed at which a cluster can erase its substructure depends on its initial virial ratio (see also Goodwin & Whitworth 2004), but also critically on the rate at which substructure evolves internally from its initial state. Dense, low-N clumps have a short internal relaxation time and will disperse rapidly (see also Kroupa & Bouvier 2003). Two-body encounters within a clump eject stars, forming a general stellar background, as well as causing clumps to increase significantly in size, making clump–clump interactions more likely, and making them more susceptible to tidal stripping. However, these effects are secondary to internal relaxation.

By considering the middle-right panel of Fig. 5 we can gauge the importance of clump merging in our simulations. The data points are from sets 3 and 4 of our parameter study. By increasing the star formation efficiency, we additionally increase the mass of the clumps. For clumps to merge, their relative impact velocities must be of the of order the velocity dispersion of the clumps. Therefore, more massive clumps should merge more easily as seen in the corresponding F09 simulations. Instead, we see the opposite – a decreasing cluster formation rate with increasing clump mass. This indicates that merging plays a minor role in the cluster formation process. Instead, it is dominated by the effects of interclump two-body encounters. For higher star formation efficiencies, the initial number of stars within a clump increases. Thus two-body encounters occur less frequently and consequently the cluster formation rate falls (as seen in the middle-right panel of Fig. 5).

The theory of clump merging developed in Fellhauer, Baumgardt, Kroupa & Spurzem (2002) and F09 is therefore not applicable in low-N ($N \sim 1000$) systems such as in the star-forming regions modelled in this study. However, in high-N systems such as mergers of clusters within cluster complexes, the effects of two-body encounters are far less important. In these scenarios, the F09 theory should remain valid.

An important conclusion to draw from this analysis is that clusters can change their appearance rapidly when they are young. A cluster that appears smooth and relaxed at an age of a few Myr may well not have formed that way. A number of authors have recently emphasized that clusters evolve rapidly and that current conditions are not always a good indicator of past conditions (e.g. Bastian et al. 2008; Allison et al. 2009).

6 SUMMARY AND CONCLUSIONS

Both observations and theory agree that stars form with a complex clumpy distribution within a star-forming region. Small clumps containing ∼tens of stars form embedded within the envelope of molecular gas from which they formed. However, observations of star clusters of $>$ a few Myr in age often show smooth, relaxed distributions (e.g. the Orion Nebula cluster at ∼3 Myr). In order for a smooth spherical star cluster to form, the star-forming region must erase its initial substructure.

We investigate the mechanisms by which substructure is erased by modelling star-forming regions using the NBODY6 code. Our stars are initially distributed in clumps, and embedded in a static potential to mimic the gravitational influence of the gas envelope on stellar dynamics. We conduct a parameter study to investigate the key parameters effecting the rate at which substructure is erased. Key parameters include the initial virial ratio of the clumps within the gas potential, the filling factor of clumps within the gas, the initial number of clumps and the star formation efficiency of the total star-forming region.

We find a number of new and different results compared to the results presented in a similar study in F09. These differences arise predominantly due to the proper treatment of two-body encounters in our simulations. Our key results may be summarized in the following.

(i) Clusters form predominantly from stars that are scattered out of clumpy substructure, and not by clump merging.

(ii) As a result, the rate at which a cluster forms is a strong function of the relaxation time within the clumps. Unlike in F09, the star formation efficiency of the region does not affect the cluster formation rate.

(iii) The initial virial ratio of the clumps is also a key parameter controlling the rate at which a cluster forms. The lower the initial virial ratio, the more rapidly substructure is erased and a cluster forms.

As interclump scattering has been demonstrated to be of such importance to cluster formation, it is vital that models considering the stellar dynamics of star-forming regions do so correctly. The use of softened gravity between stars will result in suppression of two-body encounters, and as such a key channel by which clusters form will be missed.

Furthermore, if star clusters form by scattering of stars from clumps, there is an increased likelihood that a moving subclump can leave a trail of stars which maintain a velocity signature of the clump from which they originated. Similar trails are reported in simulations of massive stars clusters within a dark matter halo (Assmann, Fellhauer & Wilkinson 2010). Such velocity structures may be observable in young clusters with the advent of *gaia*. If so, we anticipate that these observations could provide strong constraints on the recent formation history of young clusters. We defer a detailed study of this topic to a latter paper (Smith et al. 2011).

ACKNOWLEDGMENTS

MF acknowledges financial support through FONDECYT grant 1095092. RS is financed by GEMINI-CONICYT fund 32080008 and a COMITE MIXTO grant. PA is financed through a CONICYT PhD Scholarship.

REFERENCES

Aarseth S. J., 2003, Gravitational N-Body Simulations. Cambridge Univ. Press, Cambridge
Aarseth S. J., Hills J. G., 1972, A&A, 21, 255
Aarseth S. J., Henon M., Wielen R., 1974, A&A, 37, 183
Allison R. J., Goodwin S. P., Parker R. J., Portegies Zwart S. F., de Grijs R., Kouwenhoven M. B. N., 2009, MNRAS, 395, 1449
Allison R. J., Goodwin S. P., Parker R. J., Portegies Zwart S. F., de Grijs R., 2010, 407, 1098
André P., Belloche A., Motte F., Peretto N., 2007, A&A, 472, 519
André P. et al., 2010, A&A, 518, L102
Assmann P., Fellhauer M., Wilkinson M. I., 2010, in de Grijs R., Lépine J. R. D., eds, Proc. IAU Symp. 266, Star Clusters as Building Blocks for dSph Galaxy Formation. Cambridge Univ. Press, Cambridge, p. 353
Bastian N., Gieles M., Goodwin S. P., Trancho G., Smith L. J., Konstantopoulos I., Efremov Y., 2008, MNRAS, 389, 223
Bate M. R., 2009, MNRAS, 397, 232
Bate M. R., Clarke C. J., McCaughrean M. J., 1998, MNRAS, 297, 1163
Bate M. R., Bonnell I. A., Bromm V., 2003, MNRAS, 339, 577
Boffin H. M. J., Watkins S. J., Bhattal A. S., Francis N., Whitworth A. P., 1998, MNRAS, 300, 1189

Boily C. M., Clarke C. J., Murray S. D., 1999, MNRAS, 302, 399
Bonnell I. A., Bate M. R., Clarke C. J., Pringle J. E., 2001, MNRAS, 323, 785
Bonnell I. A., Bate M. R., Vine S. G., 2003, MNRAS, 343, 413
Bonnell I. A., Clark P., Bate M. R., 2008, MNRAS, 389, 1556
Bressert E. et al., 2010, MNRAS, 409, L54
Cartwright A., Whitworth A. P., 2004, MNRAS, 348, 589
Di Francesco J., André P., Myers P. C., 2004, ApJ, 617, 425
di Francesco J. et al., 2010, A&A, 518, L91
Fellhauer M., Baumgardt H., Kroupa P., Spurzem R., 2002, Celestial Mech. Dynamical Astron., 82, 113
Fellhauer M., Wilkinson M. I., Kroupa P., 2009, MNRAS, 397, 954 (F09)
Gieles M., Sana H., Portegies Zwart S. F., 2010, MNRAS, 402, 1750
Goldsmith P. F., Heyer M., Narayanan G., Snell R., Li D., Brunt C., 2008, ApJ, 680, 428
Goodwin S. P., 1998, MNRAS, 294, 47
Goodwin S. P., Whitworth A. P., 2004, A&A, 413, 929
Gouliermis D. A., Schmeja S., Klessen R. S., de Blok W. J. G., Walter F., 2010, ApJ, 725, 1717
Gutermuth R. A., Megeath S. T., Pipher J. L., Williams J. P., Allen L. E., Myers P. C., Raines S. N., 2005, ApJ, 632, 397
Gutermuth R. A. et al., 2008, ApJ, 674, 336
Gutermuth R. A., Megeath S. T., Myers P. C., Allen L. E., Pipher J. L., Fazio G. G., 2009, ApJS, 184, 18
Heggie D. C., 1974, in Kozai Y., ed., Proc. IAU Symp. 62, Stability of the Solar System and of Small Stellar Systems. Springer, New York, p. 225
Kirk H., Johnstone D., Tafalla M., 2007, ApJ, 668, 1042
Klessen R. S., Burkert A., 2000, ApJS, 128, 287
Kroupa P., 1995, MNRAS, 277, 1522
Kroupa P., Bouvier J., 2003, MNRAS, 346, 343
Moeckel N., Bonnell I. A., 2009, MNRAS, 396, 1864
Offner S. S. R., Hansen C. E., Krumholz M. R., 2009, ApJ, 704, L124
Parker R. J., Goodwin S. P., Kroupa P., Kouwenhoven M. B. N., 2009, MNRAS, 397, 1577
Peretto N., André P., Belloche A., 2006, A&A, 445, 979
Pfalzner S., Vogel P., Scharwächter J., Olczak C., 2005, A&A, 437, 967
Sánchez N., Alfaro E. J., Pérez E., 2007, ApJ, 656, 222
Smith R., Fellhauer M., Goodwin S., Assmann P., 2011, MNRAS, in press (doi:10.1111/j.1365-2966.2011.18604.x)
Testi L., Sargent A. I., Olmi L., Onello J. S., 2000, ApJ, 540, L53
Thies I., Kroupa P., Theis C., 2005, MNRAS, 364, 961
Thies I., Kroupa P., Goodwin S. P., Stamatellos D., Whitworth A. P., 2010, ApJ, 717, 577
Walsh A. J., Myers P. C., Burton M. G., 2004, ApJ, 614, 194
Walsh A. J., Myers P. C., Di Francesco J., Mohanty S., Bourke T. L., Gutermuth R., Wilner D., 2007, ApJ, 655, 958
Watkins S. J., Bhattal A. S., Boffin H. M. J., Francis N., Whitworth A. P., 1998, MNRAS, 300, 1214
Zinnecker H., 2008, in Vesperini E., Giersz M., Sills A., eds, Proc. IAU Symp. 246, On the Origin of the Orion Trapezium System. Cambridge Univ. Press, Cambridge, p. 75

This paper has been typeset from a TEX/LATEX file prepared by the author.